Green Chemistry

Accepted Manuscript

This article can be cited before page numbers have been issued, to do this please use: Z. Yaoyao, T. Rong, M. Gao, P. Hao and D. Yin, *Green Chem.*, 2016, DOI: 10.1039/C6GC02743A.

This is an Accepted Manuscript, which has been through the Royal Society of Chemistry peer review process and has been accepted for publication.

Accepted Manuscripts are published online shortly after acceptance, before technical editing, formatting and proof reading. Using this free service, authors can make their results available to the community, in citable form, before we publish the edited article. We will replace this Accepted Manuscript with the edited and formatted Advance Article as soon as it is available.

You can find more information about Accepted Manuscripts in the author guidelines.

Please note that technical editing may introduce minor changes to the text and/or graphics, which may alter content. The journal's standard Terms & Conditions and the ethical guidelines, outlined in our author and reviewer resource centre, still apply. In no event shall the Royal Society of Chemistry be held responsible for any errors or omissions in this Accepted Manuscript or any consequences arising from the use of any information it contains.

Journal Name

Green Chemistry

Dynamic Article Links ►
View Article Online
DOI: 10.1039/C6GC02743A

Cite this: DOI: 10.1039/c0xx00000x

www.rsc.org/xxxxxx

ARTICLE TYPE

Bio-inspired single-chain polymeric nanoparticles containing chiral salen Ti^{IV} complex for highly enantioselective sulfoxidation in water

Yaoyao Zhang, Rong Tan,* Mengqiao Gao, Pengbo Hao and Donghong Yin

Received (in XXX, XXX) Xth XXXXXXXXX 200X, Accepted Xth XXXXXXXXX 200X
DOI: 10.1039/b000000x

A series of bio-inspired single-chain polymeric nanoparticles (SCPNs) containing chiral salen Ti^{IV} complex in their hydrophobic cavity were constructed from the synthesized amphiphilic copolymers of poly(NIPAAm-co-*IL*/Ti(salen)) (NIPAAm, *N*-isopropylacrylamide; *IL*/Ti(salen), vinylimidazolium ionic liquid-modified chiral salen Ti^{IV} complex). These SCPNs behaved as enzyme-mimetic catalysts due to compartmentalization and site isolation, mediating enantioselective oxidation of various sulfides in water with excellent yields (90–99%) and enantioselectivities (ee, 88–99%). Especially, the ee values observed for electron-rich substrates (>95% ee) represented the best results so far in titanium-salen systems. Moreover, the catalysts could be easily recovered for steady reuse by thermo-controlled separation due to the thermo-responsive property. This work first constructed the titanium-containing biomimetic SCNPs for biocatalysis of enantioselective sulfoxidation in water.

Introduction

Asymmetric sulfoxidation catalyzed by chiral salen Ti^{IV} complex is an importance transformation in organic synthesis, since the obtained enantiopure sulfoxides are valuable chiral intermediates for synthesis of fine chemicals.[1] Although high yields of chiral sulfoxides are often achieved in organic systems, the transformation is inefficient in water due to poor water-solubility of sulfides and catalyst. As we all know, in nature, most chemical conversions are efficiently carried out in aqueous environment with the use of enzymes. Although a few are catalytic nucleic acid molecules, most enzymes are proteins, which self-fold into compartmentalized, three-dimensional structures with hydrophobic, catalytically active cores surrounded by hydrophilic shells.[2] The featured structure allows reactions to occur inside the hydrophobic compartment efficiently, while the hydrophilic shells remain compatible with aqueous environments. Inspired by enzyme catalysis, we decided to develop an enzyme-mimetic chiral salen Ti^{IV} catalyst to realize effective asymmetric sulfoxidation in water.

Folding of a single linear polymer chain into a hydrophobic-cavity-containing SCPN, which is reminiscent of the folding of proteins, has recently been realized as a feasible approach for the construction of enzyme-like comparment.[3] The obtained SCPNs often exhibit features that resemble natural enzymes. In particular, water-soluble SCPNs, in which the active sites are located in the hydrophobic core, have demonstrated enzyme-mimetic activity and selectivity in aqueous catalysis.[1d, 3b, 4] The fascinating SCPNs approach encouraged us to design Ti(salen)-containing water-soluble SCPNs as enzyme-like catalysts for efficient asymmetric sulfoxidation in water. Since amphiphilic copolymers tended to self-fold into water-soluble SCPN in water *via* an intramolecular hydrophobic interaction, as with proteins,[4] we decided to prepare a Ti(salen) containing amphiphilic copolymer precursor through the copolymerization of hydrophobic Ti(salen) with hydrophilic monomer. We envisioned that the Ti(salen) units should trigger self-folding of the amphiphiles in water through intramolecular hydrophobic interaction, forming the water-soluble SCPNs with a hydrophobic, catalytically active interior.[5] The compartmentalized SCPNs enriched catalytic motifs and substrates in confined hydrophobic interior, which hopefully not only accelerated the aqueous asymmetric sulfoxidation, but also improved the reaction selectivity. Moreover, multiple Ti(salen) motifs confined in hydrophobic core may enforce a cooperative reaction pathway favorable for asymmetric sulfoxidation, resulting in further enhanced reaction rate and higher selectivity.[6] However, the bulky polymer matrix inevitably increased local steric hindrance around Ti(salen), which limited all complexes to adopt their preferred conformation for cooperative catalysis.[6b] This problem could be well solved by introducing a flexible IL spacer between Ti(salen) unit and the polymer backbone. In addition to ensuring the necessary conformational freedom of Ti(salen), such an IL moiety with high polarity and ionic character may also stabilize the formed metallosalen active intermediates,[7] thereby further enhancing the catalytic efficiency of chiral salen Ti^{IV} catalyst. Unfortunately, water-soluble SCPNs were difficult to be recovered from water for reuse. If the

* Key Laboratory of Chemical Biology and Traditional Chinese Medicine Research (Ministry of Education); National & Local Joint Engineering Laboratory for New Petro-chemical Materials and Fine Utilization of Resources, Hunan Normal University, Changsha 410081 (P. R. China)

Fax: +86-731-8872531; Tel: +86-731-8872576; E-mail: yiyangtanrong@126.com

†Electronic Supplementary Information (ESI) available: Identity of the catalysts, detailed NMR spectra and HPLC analysis for the chiral sulfoxides. See DOI: 10.1039/b000000x/

View Article Online
DOI: 10.1039/C6GC02743A

hydrophilic corona of SCPNs is thermo-sensitive, being able to undergo hydrophilic-to-hydrophobic switch at its lower critical solution temperature (LCST), facile recovery of SCPNs can be realized.

Herein, amphiphilic random copolymers of poly(NIPAAm-co-*IL*/Ti(salen)), in which multiple chiral salen Ti^{IV} complexes were appended on linear polymeric backbone through IL linkers, were synthesized by copolymerizing *IL*/Ti(salen) with NIPAAm *via* catalytic chain transfer polymerization (CCTP) coupled with ordinary radical polymerization technique.[8] The resulted copolymers were thermo-responsive and underwent reversible single-chain self-folding in water. At reaction temperature (25 °C), they were amphiphilic and induced efficient asymmetric sulfoxidation in water *via* self-folded hydrophobic compartment around the catalytic sites, reminiscent of enzymatic catalysis. Extremely high activity (conversion>99%), chemo- (90–98%) and enantioselectivity (88–99%) were observed over a wide range of sulfides in water. After reaction, the catalysts turned to hydrophobic upon heating, allowing for facilely recovery of catalysts for steady reuse. More attractively, the activity switching was repeatable even seven heating/cooling cycles.

Results and Discussion

Preparation and Characterization of Catalysts

Enzyme catalysis is a source of inspiration for chemists who attempt to efficiently perform organic reaction in water. Compartmentalization and site isolation are the typical characteristics responsible for high efficiency demonstrated by enzymes in natural systems.[9] Water-soluble SCPNs with hydrophobic interior are structurally regarded as artificial mimics of enzymes, since they often generate compartments that express enzyme-mimetic functions.[3] Especially, if catalytically active sites were confined in their hydrophobic compartments, it would endow the SCPNs with enzyme-mimetic activity and selectivity in aqueous catalysis. With these points in mind, we decided to shield active Ti(salen) in water-soluble SCPNs compartment to fabricate a enzyme-mimetic chiral salen Ti^{IV} catalyst for aqueous asymmetric sulfoxidation. Given that water-soluble SCPNs are often prepared from amphiphilic copolymers possessing pendant groups that trigger a self-folding of the polymer,[10] a range of amphiphilic poly(NIPAAm-co-*IL*/Ti(salen)) (**$PN_x(IS)_y$**) with various amount of hydrophobic Ti(salen) pendants was decided to prepare for this fabrication. We envisioned that the Ti(salen) pendants should trigger self-folding of the amphiphilic copolymers in water *via* intramolecular hydrophobic interaction,[5] forming water-soluble SCPNs with hydrophobic Ti(salen) interior. Thermo-responsive PNIPAAM, which can undergo hydrophilic-to-hydrophobic transformation at its LCST, was incorporated in the copolymer, to allow thermo-controlled switch of copolymers between self-folding and precipitation. This switchable behavior should not only lead to an efficient asymmetric sulfoxidation in water as a result of the "biomimetic catalysis", but also allow the precipitation of catalyst for facile recovery.

The synthesis of **$PN_x(IS)_y$** was illustrated in Scheme 1. N-alkylation of vinylimidazole with the benzyl chloride group in (*R,R*)-N-(3,5-di-*tert*-butylsalicylidene)-N'-(3-*tert*-butyl-5-chloro-methyl-salicylidene)-1,2-cyclohexanediamine (CL1),[11] together with the followed $Ti(O^iPr)_4$ treatment, gave vinylimidazolium *IL*-modified chiral salen Ti^{IV} complex (*IL*/Ti(salen)). The *IL*/Ti(salen), featuring an vinyl group in one N-alkyl chain of imidazolium IL, was copolymerized with NIPAAm, providing amphiphilic random copolymers of **$PN_x(IS)_y$** (where x and y represented the repeated units number of NIPAAm and *IL*/Ti(salen), respectively). The polymerization degree of individual NIPAAm and *IL*/Ti(salen) blocks were determined in ^1H NMR spectra by comparing the signals attributable to individual blocks (NIPAAm at *ca.* 3.26 ppm assigned to CH_3-C*H*-CH_3, and *IL*/Ti(salen) at *ca.* 6.05 ppm assigned to N-C*H*-CH_2- of N-vinyl in IL) with that of end methyl group (-SH-CH_2-CH_2-CH_3, at *ca*. 1.73 ppm) (see correspondingly ^1H NMR spectra in Section 1 of ESI).

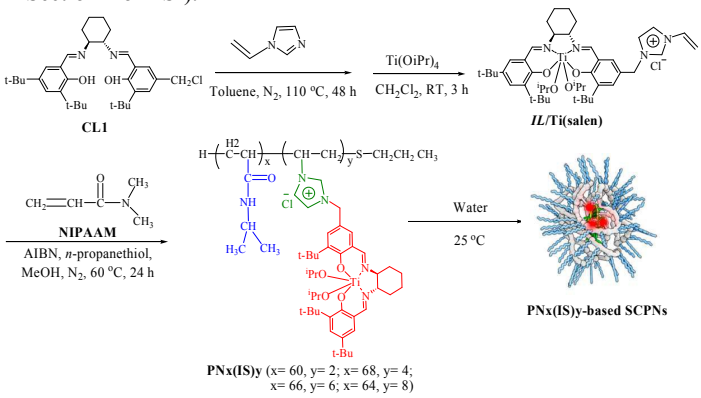

Scheme 1 Schematic representation of synthesis and self-folding of **$PN_x(IS)_y$**.

For comparison, an *IL*-free counterpart of **$PN_{68}S_4$** was also prepared according to a similar procedure, as shown in Scheme 2. During the process, (*R,R*)-N-(3,5-di-*tert*-butylsalicylidene)-N'-[3-*tert*-butyl-5-vinyl]-1,2-cyclohexanediamine (CL2)[12] was treated with $Ti(O^iPr)_4$ in dichloromethane, giving a chiral salen Ti^{IV} complex featuring a vinyl group at the 5-position. The Ti(salen) motif was used instead of *IL*/Ti(salen) to copolymerize with NIPAAm. Polymerization degrees of the individual NIPAAm and Ti(salen) blocks were also determined in ^1H NMR spectrum by comparing the signals attributable to individual blocks (NIPAAm at *ca.* 3.19 ppm assigned to CH_3-C*H*-CH_3 and Ti(salen) at *ca.* 3.41 ppm assigned to -CH-CH_2-Ph-) with that of end methyl group (-SH-CH_2-CH_2-CH_3 at *ca*. 1.72 ppm) (see Fig. S5 in Section 1 of ESI).

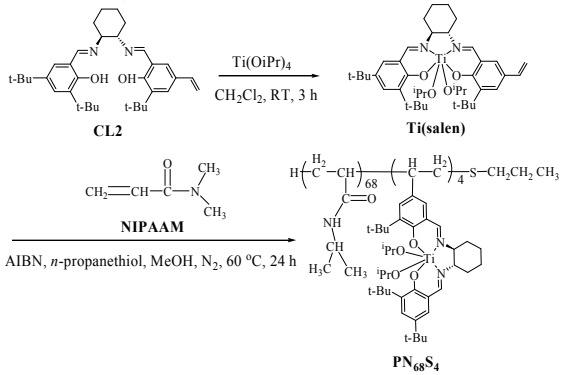

Scheme 2 Synthesis of **$PN_{68}S_4$**.

View Article Online
DOI: 10.1039/C6GC02743A

Characterization of Samples

FT-IR

The successful copolymerization of *IL*/Ti(salen) moiety with NIPAAm was verified by FT-IR. Fig. 1 showed the FT-IR spectra of typical $\mathbf{PN_{68}(IS)_4}$, as well as $\mathbf{PN_{68}S_4}$ and neat complex for comparison. Obviously, neat complex exhibited characteristic band at 1623 cm^{-1} assigned to the stretching vibration modes of C=N,[13] as well as the bands at 805 and 709 cm^{-1} associated with Ti-O bond (Fig. 1a).[14] While, these bands in $\mathbf{PN_{68}(IS)_4}$ shifted from 1623, 805 and 709 cm^{-1} to 1626, 811 and 715 cm^{-1}, respectively, compared with those in neat complex (Fig. 1b *vs*. 1a). The red shift was mainly due to the electron-deficient effect of imidazolium cation at 5-position of salen ligand.[15] The observation provided indirect proof for suspending Ti(salen) units on linear polymer backbone through an imidazolium-based IL spacer. A new characteristic band at 622 cm^{-1} associated with stretching of imidazole ring[7a] further confirmed the presence of imidazolium-based IL linkers in $\mathbf{PN_{68}(IS)_4}$ (Fig. 1b). Apart from the characteristic signal associated with Ti(salen) and IL moieties, additional bands at around 3441, 3064 and 1643 cm^{-1} were also obvious in the FT-IR spectrum of $\mathbf{PN_{68}(IS)_4}$. They were assigned to the characteristic stretching vibration of N-H of CONH, CH of CH_2-CH, and C=O of CONH in NIPAAm moiety, respectively. The observation confirmed successful incorporation of NIPAAm in $\mathbf{PN_{68}(IS)_4}$. It was the thermo-responsive NIPAAm block that ensured self-folding of copolymers in water, and also endowed the obtained SCPNs with thermo-responsive switches. As expected, $\mathbf{PN_{68}S_4}$ exhibited simialr FT-IR spectrum to $\mathbf{PN_{68}(IS)_4}$, except for the disappearance of characteristic band associated with imidazole ring (Fig. 1c *vs*. 1a). The difference was related with the absence of imidazolium-based IL linker in the $\mathbf{PN_{68}S_4}$. It was expected that the featured IL moiety would make $\mathbf{PN_{68}(IS)_4}$ more efficient and stable in the asymmetric sulfoxidation in water.

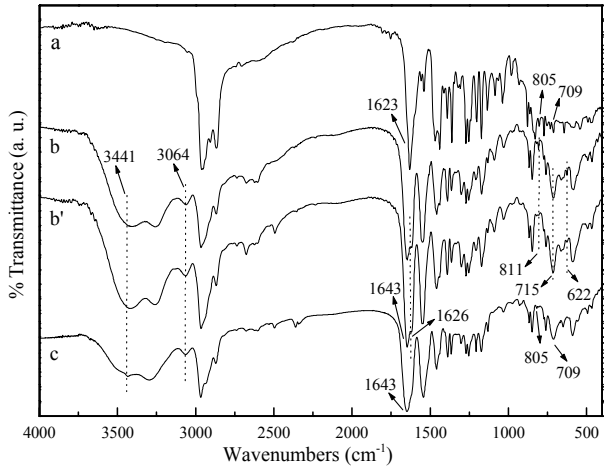

Fig. 1 FT-IR spectra of neat complex (a), fresh $\mathbf{PN_{68}(IS)_4}$ (b), recovered $\mathbf{PN_{68}(IS)_4}$ after the 7th reuse (b') and $\mathbf{PN_{68}S_4}$ (c).

TEM

The self-folding behavior of $\mathbf{PN_x(IS)_y}$ and $\mathbf{PN_{64}(IS)_8}$) in water was confirmed by TEM, as shown in Fig. 2. Obviously, the amphiphiles folded into uniform spherical nanoparticulars with average particle size of *ca*. 3 nm in water at room temperature (Fig. 2a-e). These diameter value was consistent with that adopted a single-chain folded conformation in solution.[3b,16] Notably, introducing imidazolium IL didn't significantly affect their single-chain folding behavior of $\mathbf{PN_x(IS)_y}$, since $\mathbf{PN_x(IS)_y}$–based SCPNs gave similar morphology to the SCPNs based on $\mathbf{PN_{68}S_4}$ (Fig. 2a-d vs 2e). We could thus deduced that the self-folding process of $\mathbf{PN_x(IS)_y}$ was only triggered by Ti(salen) groups, independent of the IL linkers. Logically, the hydrophobic Ti(salen) pendants avoided contacting water, inducing the self-foding of single $\mathbf{PN_x(IS)_y}$ chain into SCPNs *via* intramolecular hydrophobic interaction. High dispersion of the nanoparticulars in water implied the water-solubility of the SCPNs due to hydrophilic NIPAAm corona. Indeed, transparent solutions were observed when $\mathbf{PN_x(IS)_y}$ were dissolved in water at room temperature (Fig. 2a-e), whereas, the transparent aqueous solution turned turbid when the local temperature was heated to 35 °C, as shown by the typical $\mathbf{PN_{68}(IS)_4}$ (Fig. 2b' *vs*. 2b). The principal explanation might be that the NIPAAm conora switched from hydrophilic to hydrophobic at the higher temperature,[17] resulting in a hydrophobic state of the SCPNs. Indded, $\mathbf{PN_{68}(IS)_4}$–based SCPNs tended to gather together in water under the condition (Fig. 2b'). The thermo-sensitivity of $\mathbf{PN_x(IS)_y}$–based SCPNs in water made it possible that $\mathbf{PN_x(IS)_y}$ could be facilely recovered from the aqueous system by simple thermo-controlled separation.

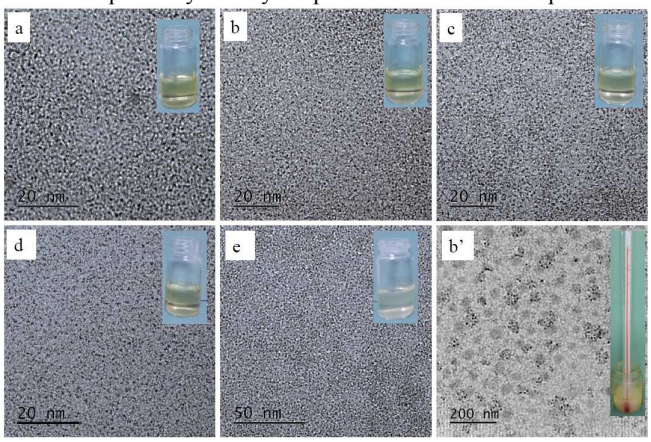

Fig. 2 TEM micrograph of self-folded $\mathbf{PN_{60}(IS)_2}$ (a), $\mathbf{PN_{68}(IS)_4}$ (b), $\mathbf{PN_{66}(IS)_6}$ (c), $\mathbf{PN_{68}(IS)_8}$ (d), and $\mathbf{PN_{68}S_4}$ (e) in water at room temperature, and self-folded $\mathbf{PN_{68}(IS)_4}$ in water at 35 °C (b') stained with phosphotungstic acid.

Cryo-TEM

Cryo-TEM was a powerful characterization technique to observe the aqueous nanoparticles, thanks to the high contrast of the nanoparticles' hard core in vitrified water. The self-folding behavior of typical $\mathbf{PN_{68}(IS)_8}$ and $\mathbf{PN_{68}S_4}$ in water was further explored by Cryo-TEM, as shown in Fig. 3. Obviously, the copolymers could be directly observed as black dots by cryo-TEM. They almost uniformly showed nanoparticles of *ca*. 4 nm diameter, without any intermolecular aggregation. The observed dots probably indicated the hydrophobic cores of the core-shell-like structures, due to the low contrast of the swollen hydrophilic shell in water. These results further demonstrated that the amphiphilic copolymers with and without IL moiety formed

View Article Online
DOI: 10.1039/C6GC02743A

single-chain nanoparticles in water (Fig. 3a vs 3b), and that there is no intermolecular aggregation. The collapse was proposed to be the result of the folding through intramolecular hydrophobic interaction of Ti(salen) pendant groups within the hydrophobic compartment.

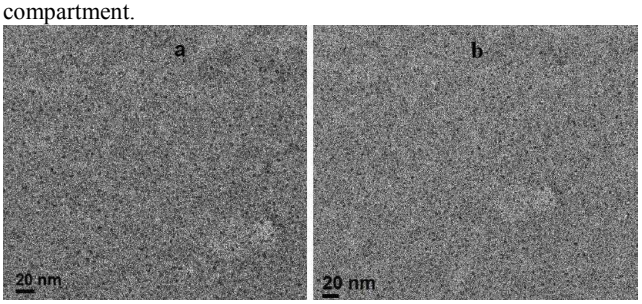

Fig. 3 Cryo-TEM images of $\mathbf{PN_{68}(IS)_4}$ (a) and $\mathbf{PN_{68}S_4}$ (b).

Circular Dichroism (CD)

The self-folding process of $\mathbf{PN_x(IS)_y}$ in water was probed in more detail by temperature-dependent Circular Dichroism (CD) spectroscopy, because of the chirality of structure-forming motif of Ti(salen) moiety. The $\mathbf{PN_x(IS)_y}$ were investigated at 10 °C intervals between 10 to 80 °C (Fig. 4). As expected, CD spectra of all $\mathbf{PN_x(IS)_y}$ showed negative Cotton effects at *ca.* 243 nm, which indicated that the copolymers formed aggregates with a preferred left-handed (M) helical sense (Fig. 4). Notably, the maximum intensity of the CD effect was significantly higher in $\mathbf{PN_{68}(IS)_4}$ (−38 mdeg) than that in $\mathbf{PN_{60}(IS)_2}$ (−18 mdeg), suggesting that the increased Ti(salen) units in copolymers enhanced the single-chain folding. It demonstrated that the Ti(salen) pendants induced the self-folding of single $\mathbf{PN_x(IS)_y}$ chain into SCPNs *via* intramolecular hydrophobic interaction. While, more number of Ti(salen) units per polymer chain lowered the intensity of Cotton effect by comparing the CD spectra of $\mathbf{PN_{66}(IS)_6}$ (−23 mdeg) and $\mathbf{PN_{64}(IS)_8}$ (−21 mdeg) with that of $\mathbf{PN_{68}(IS)_4}$ (−38 mdeg). It should be probably due to the too dense packing of bulky Ti(salen) units upon self-folding. Both observations indicated that the local Ti(salen) concentration was responsible for the magnitude of the Cotton effect and that the self-assembly occured within a single chain.

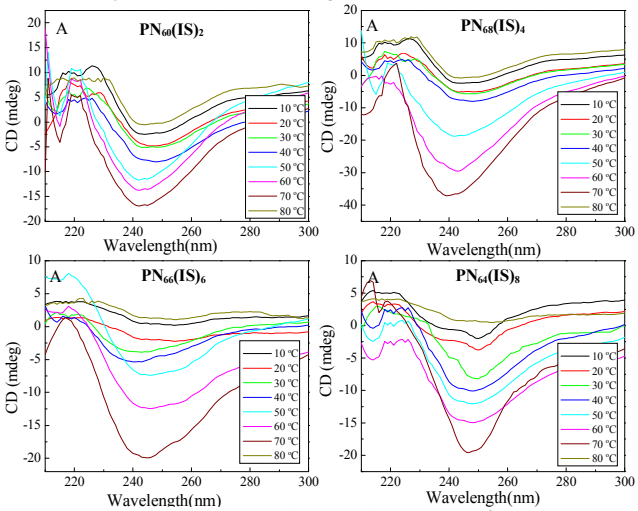

Fig. 4 CD spectra of $\mathbf{PN_x(IS)_y}$ in water from 10 to 80 °C with 10 K intervals ($\mathbf{PN_x(IS)_y}$ concentration = 0.5 g/L).

Notably, the negative Cotton effect at 243 nm increased upon heating the solution from 10 to around 70 °C, and then decreased gradually (Fig. 5). It almost disappeared at 80 °C. This indicated that the self-folding behaviors of $\mathbf{PN_x(IS)_y}$ was related to the local temperature. In fact, the solution finally turned turbid due to the lower critical solution temperature (LCST) of the copolymers above 80 °C. Full reversibility without hysteresis was observed upon slow cooling (Fig. 5). These results indicated that the polymers folded and unfolded reversibly by controlling the temperature due to the temperature-dependent water-solubility of NIPAAm units.

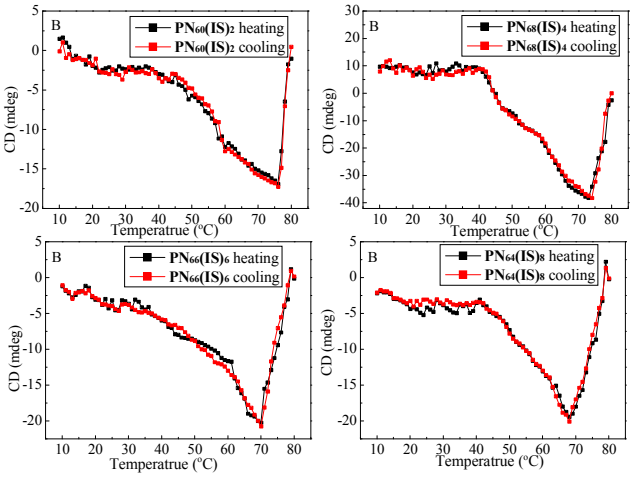

Fig. 5 Temperature-dependent CD heating-cooling curves of $\mathbf{PN_x(IS)_y}$ monitored at λ = 243 nm in water at temperatures range from 10 to 80 °C (heating rate= 1 °C /min; cooling rate= -1 °C/min), ($\mathbf{PN_x(IS)_y}$ concentration = 0.5 g/L)

Particle Size Distribution Analysis

Dynamic light scattering (DLS) was used to further determine the hydrodynamic diameter and size distribution of self-folded $\mathbf{PN_x(IS)_y}$ at room temperature (Fig. 6). The hydrodynamic diameter analysis by DLS gave monomodal symmetrical distributions with low polydispersity index (PDI) for $\mathbf{PN_{60}(IS)_2}$, $\mathbf{PN_{68}(IS)_4}$, $\mathbf{PN_{66}(IS)_6}$, and $\mathbf{PN_{64}(IS)_8}$ (0.395, 0.267, 0.315, and 0.206, respectively). It indicated the homogeneous distribution, spherical morphology, and uniform sizes of corresponding SCPNs (Fig. 3).[18] Although similar morphology, the size of SCPNs gradually decreased with increasing the content of hydrophilic Ti(salen) block in copolymer. The hydrodynamic diameter of $\mathbf{PN_{60}(IS)_2}$, $\mathbf{PN_{68}(IS)_4}$, $\mathbf{PN_{66}(IS)_6}$, and $\mathbf{PN_{64}(IS)_8}$ was *ca.* 15.8, 11.9, 8.8, and 6.5 nm, respectively. Reduced sizes were mainly due to the enhanced intramolecular hydrophobic interaction arisen from increased Ti(salen) pendants, which resulted in the more contracted conformation of SCPNs.[19] Notably, although the nanostructures were both in hydrated state, the sizes for SCPNs determined by DLS were larger than from Cryo-TEM, as typical by as shown by the typical $\mathbf{PN_{68}(IS)_4}$. It was probably due to the low contrast of the swollen hydrophilic shell in vitrified water in Cryo-TEM images.

View Article Online
DOI: 10.1039/C6GC02743A

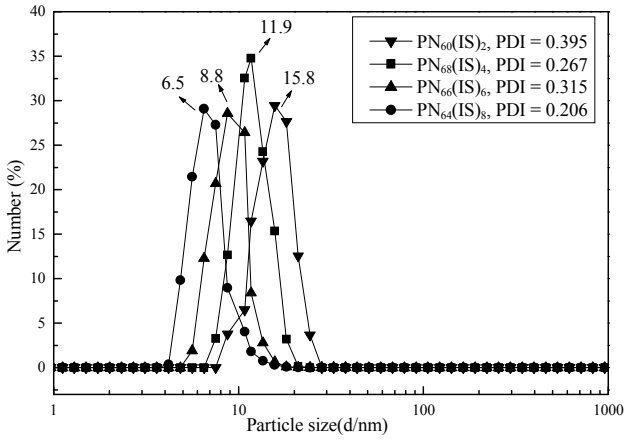

Fig. 6 Size distribution of self-folded $\mathbf{PN_x(IS)_y}$ in water at a concentration of 0.5 mg/mL at room temperature.

Catalytic Performances

As expected, the enzyme-mimetic SCPNs were capable of significantly accelerating asymmetric sulfoxidation in water with excellent selectivity, especially, rendering the reaction highly enantioselective, as shown in Table 1. Only 0.5 mol% loading of catalysts were sufficient to give excellent conversion (85-99%) of methyl phenyl sulfide with remarkable chemo (89-95%) and enantioselectivity (95-98%) in 60 min (Table 1, entries 1-4). In contrast, traditional chiral ((*R,R*)-salen)$Ti^{IV}(O^iPr)_2$ complex (neat complex, neat-C)[14] gave 48% of conversion with disappointing selectivity (65% of chemoselectivity and 76% of ee value) under identical conditions (Table 1, entry 7). The discrepancy in catalytic efficiency demonstrated the advantage of biocatalysis approach. Apart from shielding catalytic sites from surrounding aqueous environment, the compartmentalized SCPNs effectively concentrated the substrates within catalytic core, enhancing reaction rates and selectivity for the aqueous sulfoxidation.[20] In addition, multiple Ti(salen) catalytic sites confined in the hydrophobic core may enforce an intramolecular, cooperative reaction pathway resulting in enhanced reaction rates and higher selectivities.[6] Furthermore, excess aqueous H_2O_2 would be excluded from the hydrophobic reaction space, which thus minimized the undesired over-oxidation of sulfoxide to sulfone and maximized the selectivity to chiral sulfoxide. Notably, $\mathbf{PN_{68}(IS)_4}$ showed the highest catalytic efficiency in the aqueous asymmetric sulfoxidation of methyl phenyl sulfide, giving almost quantitative yield (95%) of (*R*)-sulfoxide with up to 98% ee value (Table 1, entry 2). Less number of Ti(salen) units per polymer chain ($\mathbf{PN_{60}(IS)_2}$) was undesirable for this transformation due to lower local concentration of Ti(salen) units in compartmentalized SCPNs (Table 1, entry 1). While, $\mathbf{PN_{66}(IS)_6}$ and $\mathbf{PN_{64}(IS)_8}$ with more number of Ti(salen) units per polymer chain were also detrimental to the catalysis, since too dense packing of Ti(salen) units confined in SCPNs should restrict all Ti(salen) to adopt their preferred conformation for cooperative catalysis (Table 1, entries 3 and 4).[21]

In addition to the fascinating "confined catalysis", the higher efficiency of $\mathbf{PN_x(IS)_y}$ should also relate to the flexible IL linker. An *IL*-free analog of $\mathbf{PN_{68}S_4}$, in which multiple chiral salen Ti^{IV} complexes were appended directly on the linear polymer backbone, was prepared as control catalyst to investigate the effect of IL spacer. As expected, although it had similar compartmental structure, $\mathbf{PN_{68}S_4}$ was less active and selective than *IL*-tagged $\mathbf{PN_{68}(IS)_4}$ (Table 1, entry 5 *vs*. 2). A conversion of 89% of sulfide with only 92% chemoselectivity and 95% ee was obtained over $\mathbf{PN_{68}S_4}$ under identical conditions (Table 1, entry 5). Logically, the flexible IL linker that placed the chiral complexes away from the polymer backbone ensured preferred conformation of Ti(salen) in $\mathbf{PN_{68}(IS)_4}$. This was crucial for the effective cooperative catalysis as otherwise selectivity will be lost.[6b] In addition to the conformational freedom, the *IL*-tagged $\mathbf{PN_{68}(IS)_4}$ also benefited from the local catalyst microenvironment created by the IL spacer, since the IL moiety was encapsulated in SCPNs compartment along with Ti(salen) units. The unique solvent power of encapsulated IL made $\mathbf{PN_{68}S_4}$-based SCPNs more compatible with organic sulfides and *aq*. H_2O_2,[22] increasing the concentrations of reactants in compartmentalized SCPNs. Furthermore, the polarity and ionic property of RTILs played positive effect on stabilizing the active metallosalen intermediate in the asymmetric sulfoxidation.[7] Indeed, midway addition of 1-methyl-3-buthylimidazolium chlorine IL (equivalent to the IL amount in $\mathbf{PN_{68}(IS)_4}$) into the $\mathbf{PN_{68}S_4}$-mediated sulfoxidation system increased the conversion (from 89 to 93%) and selectivity (93% of chemoselectivity and 96% of ee value) (Table 1, entry 6 *vs.* 5). While, the reactivity was still lower than that obtained over $\mathbf{PN_{68}(IS)_4}$ (Table 1, entry 6 *vs*. 2). It was reasonable that, unlike the IL in $\mathbf{PN_{68}(IS)_4}$, the small amount of IL added in $\mathbf{PN_{68}S_4}$ system was hard to be entirely encapsulated in the hydrophobic domain along with Ti(salen) motif. The results supported our hypothesis that $\mathbf{PN_{68}(IS)_4}$-mediated sulfoxidations took place within the hydrophobic compartment of SCPNs.

The advantage of SCPNs approach over $\mathbf{PN_{68}(IS)_4}$, along with the remarkable activity and selectivity, was also noticeable for other aryl methyl sulfides, such as methyl *p*-bromophenyl sulfide, methyl *p*-methoxyphenyl sulfide, methyl *p*-nitrophenyl sulfide, and methyl *o*-methoxyphenyl sulfide. All the aryl methyl sulfides get quantitatively oxidized to the corresponding sulfoxides with excellent chemo- (90-98%) and enantioselectivity (88-99%) within 90 min in water with the employment of $\mathbf{PN_{68}(IS)_4}$ (Table 1, entries 2, 9, 14, 18, and 23). The enantioselectivity was even higher than that obtained over our reported micelle-bound chiral salen Ti^{IV} catalyst (ee value, 74-95%),[6c] although the micelle-bound system also provided a confined reaction environment. Higher chiral induction for $\mathbf{PN_{68}(IS)_4}$ should benefit from the positive effect of imidazolium IL moiety confined in SCPNs, as well as more stable structure of the self-folded SCPNs than previous micelle-bound system which was dynamic in nature.[23] Notably, almost quantitative chiral induction to (*R*)-sulfide (>99%) was observed for the methyl *p*-bromophenyl sulfide and methyl *o*-methoxyphenyl sulfide over $\mathbf{PN_{68}(IS)_4}$ (Table 1, entries 9 and 23). The chemoselectivity was also unusually high with regard to the literature results.[1]

View Article Online
DOI: 10.1039/C6GC02743A

Table 1 Results of asymmetric sulfoxidation of methyl aryl sulfides over different chiral salen Ti^{IV} catalysts in water [a]

Entry	Catalyst	Substrate	T (min)	Conv. [b] (%)	Sel. [b] (%)	ee [c] (%)
1	**$PN_{60}(IS)_2$**		60	85	89	95
2	**$PN_{68}(IS)_4$**		60	99	95	98
3	**$PN_{66}(IS)_6$**		60	96	93	97
4	**$PN_{64}(IS)_8$**		60	93	93	97
5	**$PN_{68}S_4$**		60	89	92	95
6	**$PN_{68}S_4$** [d]		60	93	93	96
7	neat-C		60	48	65	76
8	**$PN_{68}(IS)_4$**	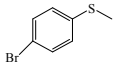	60	88	94	>99
9	**$PN_{68}(IS)_4$**		80	99	92	>99
10	**$PN_{68}S_4$**		60	75	90	98
11	**$PN_{68}S_4$** [d]		60	80	92	98
12	neat-C		60	59	78	81
13	**$PN_{68}(IS)_4$**	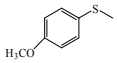	60	96	95	94
14	**$PN_{68}(IS)_4$**		65	99	94	95
15	**$PN_{68}S_4$**		60	91	87	90
16	**$PN_{68}S_4$** [d]		60	94	90	92
17	neat-C		60	62	81	45
18	**$PN_{68}(IS)_4$**	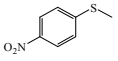	45	99	98	88
19	**$PN_{68}S_4$**		45	85	96	84
20	**$PN_{68}S_4$** [d]		45	89	97	85
21	neat-C		45	51	87	56
22	**$PN_{68}(IS)_4$**	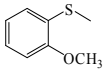	60	78	90	99
23	**$PN_{68}(IS)_4$**		90	99	90	99
24	**$PN_{68}S_4$**		60	70	87	99
25	**$PN_{68}S_4$** [d]		60	72	88	98
26	neat-C		60	40	75	67

[a] Catalyst (0.5 mol% of substrate, based on titanium content), substrate (1.0 mmol), H_2O_2 (1.2 mmol, added within 15 min), deionized water (1 mL), 25 °C. [b] Determined by GC. [c] Determined by HPLC (Daicel chiralpak AD column). [d] **$PN_{68}S_4$** (0.5 mol% of substrate, based on titanium content), 1-methyl-3-buthylimidazolium chlorine (0.001 g, equivalent to the amount of IL in **$PN_{68}(IS)_4$**), substrate (1.0 mmol), H_2O_2 (1.2 mmol, added in 15 min), water (1 mL), 25 °C.

To further confine the universality of **$PN_{68}(IS)_4$**, a batch of alkyl phenyl sulfides with various length of the alkyl chain (C1, C2, C4, and C6) was synthesized and subjected to the sulfoxidation conditions. As expected, all the alkyl phenyl sulfides also get quantitatively oxidized to the corresponding sulfoxides in water with excellent selectivity with the employment of **$PN_{68}(IS)_4$** (Table 2). Interestingly, we noticed that increasing the length of alkyl chain in sulfides led to the enhanced reaction rate and improved selectivity (in terms of chemo- and enantioselectivity). The asymmetric sulfoxidation of methyl phenyl sulfide was complete in 60 min, giving 95% chemoselectivity and 98% ee value (Table 2, entry 1). As the number of carbon atoms of alkyl chain increased from 1 to 2, 4 and further to 6, the catalytic efficiency and selectivity increased accordingly (Table 2, entries 2, 3, and 4 *vs.* entry 1)). In particular, the *n*-hexyl phenyl sulfide was almost quantitatively converted to (*R*)-*n*-hexyl phenyl sulfoxide within 50 min (99% chemoselectivity and 99% ee value) (Table 2, entry 4). The enhanced catalytic efficiency should arise from the increased hydrophobicity of sulfides with the increase of alkyl chains length. The results indicated that the hydrophobicity of the reactants was driving force of asymmetric sulfoxidation using **$PN_{68}(IS)_4$**. Logically, the more hydrophobic the sulfide, the better is the diffusion of sulfide into the hydrophobic core of the SCPNs where the catalytic active centers are located.

Table 2 Results of asymmetric sulfoxidation of alkyl phenyl sulfides over **$PN_{68}(IS)_4$** in water [a]

Entry	Substrate [b]	T (min)	Conv. [c] (%)	Sel. [c] (%)	ee [d] (%)
1	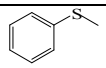	60	>99	95	98
2	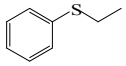	60	>99	97	>99
3	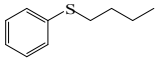	55	>99	>99	>99
4	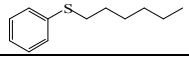	50	>99	>99	>99

[a] **$PN_{68}(IS)_4$** (0.5 mol% of substrate, based on titanium content), substrate (1.0 mmol), H_2O_2 (1.2 mmol, added within 15 min), deionized water (1 mL), 25 °C. [b] The alkyl phenyl sulfides were synthesized according to reference [24], and identified by NMR available in the Supporting Information. [c] Determined by GC. [d] Determined by HPLC (Daicel chiralpak AD column).

Kinetics was used to further investigate the advantages of SCPNs approach in aqueous catalysis, as well as the positive effect of IL moiety on catalytic performance. The corresponding kinetic curves and rate curves were shown in Fig. 7. Obviously, **$PN_{68}(IS)_4$** showed gradient increase in conversion of sulfide in corresponding kinetic curves, when asymmetric sulfoxidation was performed in water (Fig. 7A-a). The corresponding observed rate constant (k_{obs}) initially rose rapidly due to the dramatically increasing concentration of substrate in hydrophobic compartments, went through a maximum, and then drastically decreased due to a dilution effect (Fig. 7B-a).[25] The featured kinetics demonstrated confined catalysis of asymmetric sulfoxidation in water over compartment. To further evaluate the importance of compartmentalization, we carried out the reaction with **$PN_{68}(IS)_4$** in dichloromethane, a solvent in which **$PN_{68}(IS)_4$** could also be well dissolved. As expected, at the same catalyst concentration, **$PN_{68}(IS)_4$** was far less efficient than in water (Fig. 7d *vs*. 7a). In fact, self-folding of **$PN_{68}(IS)_4$** into SCPNs didn't occur when reaction was performed in dichloromethane. Amphiphilic **$PN_{68}(IS)_4$** just located at the interface between dichloromethane and water (aqueous H_2O_2) in the biphasic system, behaving as a common phase-transfer catalyst, rather than a concentrator. Lower local concentration of substrates and catalytic species in the biphasic system was insufficient for efficient catalysis. The results were consistent with our hypothesis that high local concentration of catalytic species was crucial for this system to be active, and this was only achieved in the folded state and in the presence of structured hydrophobic compartments. For this reason, it was not surprising that traditional neat complex gave the lowest k_{obs} in water due to poor solubility of catalyst and sulfides in water (Fig. 7e). These results

View Article Online
DOI: 10.1039/C6GC02743A

confirm that $\mathbf{PN_{68}(IS)_4}$ created a more favourable microenvironment for sulfoxidation in water than in organic solvent. Moreover, despite also SCPNs catalysis, the k_{obs} over $\mathbf{PN_{68}S_4}$ was always lower than that over $\mathbf{PN_{68}(IS)_4}$ in the aqueous sulfoxidation (Fig. 7b *vs*. 7a), and simple addition of IL into the $\mathbf{PN_{68}S_4}$ system accelerated the reaction (Fig. 7c *vs*. 7b). The observations did agree with the active role of imidazolium-based IL in the overall reaction mechanism. Furthermore, we noticed that the SCPNs-based sulfoxidation started after 35-40 min (Fig. 7a-c). The delayed reaction should be probably due to that the compartmentalized structure of SCPNs somewhat hindered the permeation of substrates into hydrophobic interior.[26] The observations provided further evidence for the confined catalysis in SCPNs compartment.

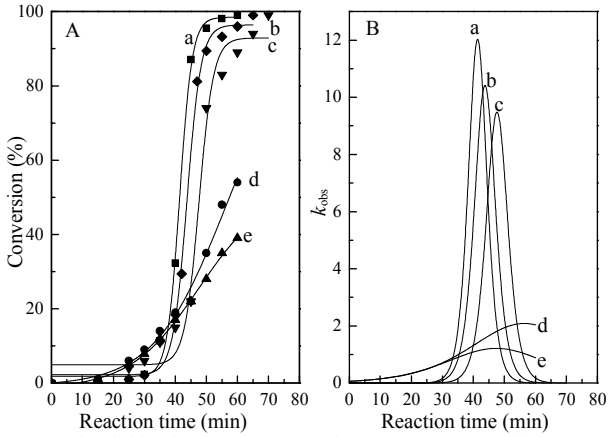

Fig. 7 Fitted kinetic curves (A) and rate curves (B) of asymmetric sulfoxidation of methyl phenyl sulfide over $\mathbf{PN_{68}(IS)_4}$ (a), $\mathbf{PN_{68}S_4}$ together with 1-methyl-3-buthylimidazolium (b), $\mathbf{PN_{68}S_4}$ (c), and neat complex (e) in water, and over $\mathbf{PN_{68}(IS)_4}$ in dichloromethane (d).

Aside from exhibiting enzyme-mimetic activity and selectivity, $\mathbf{PN_x(IS)_y}$ exhibited the reversibility of thermal driven water-solubility switching. Water-solubility switching process was determined by monitoring the optical transmittance of $\mathbf{PN_x(IS)_y}$ solution at 450 nm using UV-vis spectrophotometry (Fig. 8). Clear solutions of the $\mathbf{PN_x(IS)_y}$ in water were observed at 15 ^oC. After being heated to 80 ^oC, the transmittance decreased dramatically, which was corresponding to the water-solubility switch from amphiphilic to hydrophobic. By continuous cooling to 15 ^oC, the solutions reverted to the initial clear state. Significantly, the reversible transition between turbidity and clarity could repeat several times, indicating the good thermal responsiveness of the supramolecular assembly. The salient features allowed for facile recovery of $\mathbf{PN_x(IS)_y}$ from the aqueous phase by thermo-controlled separation.

Fig. 9 gave the reusability of $\mathbf{PN_x(IS)_y}$ in asymmetric oxidation of methyl phenyl sulfide in water. To our delight, the catalysts could be reused up to seven times without significant loss in activity and selectivity. Leaching tests of catalysts revealed negligible leaching loss of titanium species (less than 0.1 ppm by ICP) to reaction medium during the oxidation. Chemical analysis of the recovered catalysts gave titanium content (0.449, 0.503, 0.521, and 0.562 mmol/g for recovered $\mathbf{PN_{60}(IS)_2}$, $\mathbf{PN_{68}(IS)_4}$, $\mathbf{PN_{66}(IS)_6}$, and $\mathbf{PN_{64}(IS)_8}$, respectively) almost identical to that of the corresponding fresh one. Furthermore, no significant change of catalysts took place even after reuse for seven times, as shown by FT-IR spectra of the fresh and recovered typical $\mathbf{PN_{68}(IS)_4}$ (Fig. 1b *vs*. 1b'). It suggested the perfect stability of $\mathbf{PN_x(IS)_y}$ in aqueous asymmetric sulfoxidation. Oxidative decomposition of chiral salen Ti^{IV} complex, a main reason for deactivation of the catalyst in H_2O_2-based oxidation,[27] did not occur during the reaction. The excellent stability of catalysts should arise from the shielding of chiral salen Ti^{IV} complex in a hydrophobic pocket, which protected Ti(salen) complex from oxidative decomposition by excluding excess H_2O_2 from the complex. Furthermore, imidazolium IL moiety incorporated in the hydrophobic pocket also played a positive effect on stabling the complex.[7]

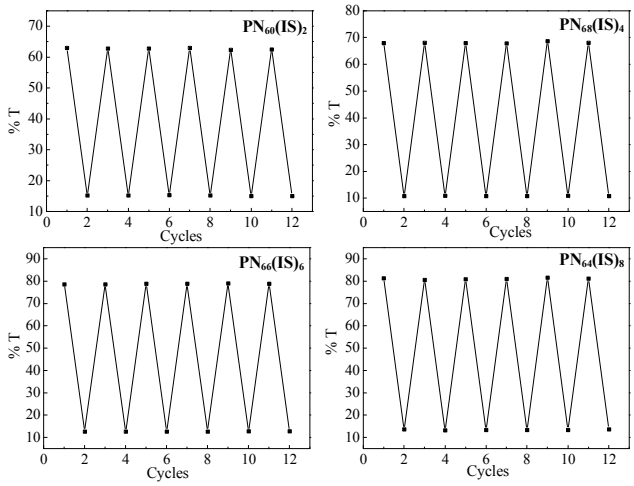

Fig. 8 Optical transmittance at 450 nm of $\mathbf{PN_x(IS)_y}$ solution observed upon several cycles under heating at 80 ^oC and then cooling to 15 ^oC

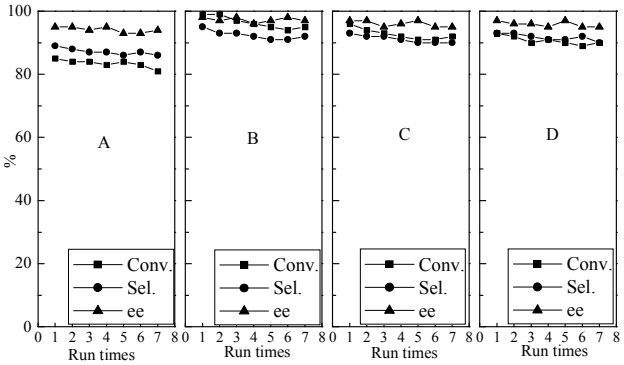

Fig. 9 Reuse of $\mathbf{PN_{60}(IS)_2}$ (A), $\mathbf{PN_{68}(IS)_4}$ (B), $\mathbf{PN_{66}(IS)_6}$ (C) and $\mathbf{PN_{64}(IS)_8}$ (D) in asymmetric sulfoxiation of methyl phenyl sulfide in water.

Conclusions

A novel series of enzyme-inspired SCPNs which contained chiral salen Ti^{IV} complex in the hydrophobic core was constructed for asymmetric sulfoxidation in water. The SCPNs demonstrated enzyme-mimetic activity and selectivity for a wide range of methyl aryl sulfides in water due to the compartmentalization and the effective shielding of active sites from the aqueous environment. In particular, the enantioselectivity observed for electron-rich substrates represented the best results so far in titanium-salen systems. More interestingly, the catalysts could be facilely recovered from the aqueous system for efficient reuse by adjusting local temperature.

View Article Online
DOI: 10.1039/C6GC02743A

The high activity and selectivity, as well as outstanding reusability, made the enzyme-inspired SCPNs highly promising for biocatalysis of various organic reactions in water. Furthermore, the SCPNs approach also inspired researchers to perfect the design and synthesis of other enzyme mimics and to tailor their functionality for a much wider range of applications.

Experimental Section

Materials and Reagents

N,N-Azobis(isobutyronitrile) (AIBN), NIPAAm, *n*-propanethiol, and L(+)-tartaric acid were purchased from Acros. Tetra-isopropyl titanate, vinylimidazole and aryl methyl sulfides were obtained by J&K. 2-tert-Butyl phenol was purchased from Alfa Aesar. Other commercially available chemicals were laboratory grade reagents from local suppliers. All solvents were purified by standard procedures. AIBN was recrystallized from methanol. NIPAAm was purified by recrystallization from *n*-hexane and dried in vacuo.

Methods

FT-IR spectra were obtained as potassium bromide pellets with a resolution of 4 cm^{-1} and 32 scans in the range 400– 4000 cm^{-1} using an AVATAR 370 Thermo Nicolet spectrophotometer. NMR of samples was recorded at a BRUKER AVANCE -500 spectrometer with TMS as an internal standard. TEM images were obtained on a Microscope Tecnai F20 at an accelerating voltage of 200 kV. Samples were prepared by depositing aqueous solution (0.5 mg· mL^{-1}) onto a carbon-coated copper grid, followed by removal of excess solution by blotting the grid with filter paper. The samples were dried for 72 h at room temperature in a desiccator. After that, the samples were negatively stained by phosphotungstic acid and dried for another 72 h before examination. Cryo-TEM measurements were performed on a FEI Technai 20, type Sphera. The Technai 20 is equipped with a LaB6 filament operating at 200 kV and the images were recorded using a 1k x 1k Gatan CCD camera. The sample vitrification procedure was carried out using an automated vitrification robot (FEI Vitrobot™ Mark III). CryoTEM grids, R2/2 Quantifoil Jena grids, were purchased from Quantifoil Micro Tools GmbH. The grids underwent a surface plasma treatment using a Cressington 208 carbon coater operating at 5 mA for 40 s, prior to the vitrification procedure that was carried out within the environmental chamber of the VitrobotTM at room temperature (1 mg/mL polymer solution in H_2O, 3 µL aliquots, 3 s blotting time, -2 mm blotting offset, 100 % relative humidity). The vitrified specimens were stored under liquid nitrogen. Molecular weight and molecular-weight distribution of the synthesized copolymers was obtained by gel permeation chromatography (GPC). Analyses were performed on an Alltech Instrument (Alltech, America) using THF as the solvent eluting at a flow of 1 mL min^{-1} through a Jordi GPC 10 000 A column (300 mm × 7.8 mm) equipped with an Alltech ELSD 800 detector. The system was calibrated with standard polystyrenes. The detection temperature is 40 °C and column temperature is 30 °C. CD measurements were performed on a MOS-500 spectropolarimeter where the sensitivity, time constant and scan rate were chosen appropriately (sensitivity: standard; response: 2 s; band width: 1 nm; data pitch: 0.1 nm; scanning speed: 20 nm/min). Corresponding temperature-dependent measurements were performed with a PFD-425S/15 Peltier-type temperature controller with a temperature range of 10–80 °C and adjustable temperature slope, in all cases temperature slope of 1 °C /min was used. DLS was performed using a ZS90 Laser Particle Size Analyzer (Malvern, UK). The sample solutions for measurements were prepared for concentrations of 0.5 mg· mL^{-1} followed by filtering through a 0.45 lm disposable polyamide membrane to free it from dust particles. The content of titanium contents in the samples was determined by inductively coupled plasma mass spectrometry (ICP-MS) on a NexION 300X analyzer (Perkin-Elmer Corp.). Optical rotation of samples was measured in dichloromethane on a WZZ-2A Automatic Polarimeter. The surface tension of an aqueous solution of catalyst was measured as a function of catalyst concentration on a Krüss K12 tensiometer using the Wilhelmy plate method at 25 °C. The surface tension vs. catalyst concentration plot gives information on the critical micelle concentration (CMC). HPLC analyses were performed on a TECHCOMP L2000 or JASCO 2089 liquid chromatograph using the Daicel chiralpak AD column.

Preparation of Catalysts

Synthesis of IL/Ti(salen): The asymmetric chiral salen ligand (CL1, 3.2 mmol, 1.725 g) was mixed with vinyl imidazole (3 mmol, 0.28 g) in dry toluene (15 mL). The mixture was refluxed for 48 h under nitrogen protection, and then concentrated in vacuo. The residue was dissolved in dichloromethane, and followed by treatment with $Ti(O^iPr)_4$ (3.2 mmol, 0.91 g) for 3 h at room temperature. After removal of solvent, the crude product was treated with water (100 mL), filtered, and washed with water and *n*-hexane. The crude product was dissolved in CH_2Cl_2 and filtered to remove any traces of TiO_2. The filtrate was concentrated in vacuum and further dried in vacum at 40 °C overnight, giving yellow powder of *IL*/Ti(salen). *IL*/Ti(salen): FT-IR (KBr): γ_{max}/cm^{-1} 3437, 3310, 3073, 2973, 2933, 2882, 1653, 1540, 1458, 1384, 1365, 1263, 1172, 1130, 1051, 986, 922, 881, 838, 626, 518 cm^{-1}. ^1H NMR (500 MHz, CD_3Cl_3): δ 8.11~7.65(s, 2 H, C*H*=N), 7.18~7.59 (m, 4 H, Ar*H*), 6.05 (m, 1 H, N-C*H*=CH_2) 4.15 (s, 1H, C=NC*H*), 3.87(m, 1 H, C=NC*H*), 3.56 (m, 4 H, N-CH=CH_2 and -N-CH_2-N-), 2.36~2.65 (m, 2 H, CH_3-C*H*-CH_3 in ^{i}PrO-), 1.46 (m, 8 H, cyclohexyl-*H*), 1.23~1.37 (m, 27 H, *H*- in t-butyl), 1.31(m, 12 H, CH_3-CH-CH_3 in ^{i}PrO-).

Preparation of $PN_x(IS)_y$: Monomers of NIPAAm and *IL*/Ti(salen) with various molar feed (9.0 mmol of NIPAAm and 0.3 mmol of *IL*/Ti(salen) for **$PN_{60}(IS)_2$**, 9.0 mmol of NIPAAm and 0.5 mmol of *IL*/Ti(salen) for **$PN_{68}(IS)_4$**, 9.0 mmol of NIPAAm and 0.8 mmol of *IL*/Ti(salen) for **$PN_{66}(IS)_6$**, 8.8 mmol of NIPAAm and 1.0 mmol of *IL*/Ti(salen) for **$PN_{64}(IS)_8$**) were dissolved in dry methanol (20 mL) in Schlenk tube. *n*-Propanethiol (chain transfer reagent, 1 mmol, 0.076 g) and AIBN (radical initiator, 0.5 mmol, 0.082 g) were then added into the solutions. The reaction mixtures were degassed by bubbling with nitrogen gas at room temperature for 30 min. Polymerizations were carried out at 60 °C for 24 h under nitrogen gas atmosphere. After being cooled to room temperature, the mixtures were concentrated under vacuum. Crude products were purified by dialysis in THF. **$PN_x(IS)_y$** were precipitated in diethyl ether as yellow powders (where x and y represented the repeated units number of NIPAAm and *IL*/Ti(salen), respectively; the number was determined by ^1H NMR spectra of corresponding copolymers, see Section S1 in ESI). Different molar feed ratio of 9.0/0.3, 9.0/0.5, 9.0/0.8, and 8.8/1.0 resulted in the copolymers of **$PN_{60}(IS)_2$, $PN_{68}(IS)_4$, $PN_{66}(IS)_6$,** and **$PN_{64}(IS)_8$**, respectively.

$PN_{60}(IS)_2$: FT-IR (KBr): γ_{max}/cm^{-1} 3436, 3313, 3075, 2971, 2942, 2891, 1653, 1542, 1457, 1386, 1368, 1263, 1170, 1131, 1054, 927, 880, 836, 806, 709, 624, 519 cm^{-1}. ^1H NMR (500 MHz, $CDCl_3$): δ 6.24~6.89 (m, 60 H, HC-N*H*-C=O), 6.08 (m, 2 H, N-C*H*-CH_2- of N-vinyl), 4.18 (m, 2 H, C=NC*H*), 3.99 (m, 60 H, -C*H*-CH_2 in NIPAAm), 3.88 (m, 2 H, C=NC*H*), 3.67 (m, 8 H, -CH-CH_2- of N-vinyl in IL and -N-CH_2-N-), 3.45 (m, 60 H, CH_3-C*H*-CH_3 in NIPAAm), 3.06 (m, 12 H, -N-CH_2-CH_2-N-

View Article Online
DOI: 10.1039/C6GC02743A

and -N-CH_2-Ph-), 2.84 (m, 2 H, SH-CH_2-CH$_2$-CH$_3$), 2.64~2.73 (m, 4 H, CH$_3$-CH-CH$_3$ of ^{i}PrO- in Ti(salen)), 2.38 (m, 2 H, SH-CH$_2$-CH_2-CH$_3$), 1.86~2.12 (m, 120 H, -CH_2-CH- in NIPAAm), 1.71(s, 3 H, SH-CH$_2$-CH$_2$-CH_3), 1.43 (16 H, cyclohexyl-*H*), 1.13~1.33 (54 H, *H*- in t-butyl), 1.09~1.16 (m, 384 H, CH_3-CH-CH_3 in ^{i}PrO- and NIPAAm). GPC (THF): *Mn* = 8990, *Mw* = 12840, PDI = 1.43. α_{25}^D = -16.0 (C = 0.005 g/mL, CH_2Cl_2), titanium content: 0.452 mmol.g^{-1}.

PN$_{68}$(IS)$_4$: FT-IR (KBr): γ_{max}/cm^{-1} 3436, 3302, 3064, 2967, 2923, 2867, 1645, 1541, 1454, 1382, 1365, 1265, 1175, 1128, 1053, 920, 882, 834, 809, 709, 635, 624, 509 cm^{-1}. ^{1}H NMR (500 MHz, CD_3Cl_3): δ 8.15~7.68 (m, 8 H, C*H*=N), 7.14~7.64 (m, 16 H, Ar*H*), 6.24~6.89 (m, 68 H, HC-N*H*-C=O), 6.05 (m, 4 H, N-C*H*-CH$_2$- of N-vinyl), 4.14 (m, 4 H, C=NC*H*), 3.99 (m, 68 H, -C*H*-CH$_2$- in NIPAAm), 3.85(m, 4 H, C=NC*H*), 3.58 (m, 16 H, -CH-CH_2- of N-vinyl in IL and -N-CH_2-N-), 3.26 (m, 68 H, CH$_3$-C*H*-CH$_3$ in NIPAAm), 2.90 (m, 24 H, -N-CH_2-CH_2-N- and -N-CH_2-Ph-), 2.78(m, 2 H, SH-CH_2-CH$_2$-CH$_3$), 2.34~2.68 (m, 8 H, CH$_3$-C*H*-CH$_3$ of ^{i}PrO- in Ti(salen)), 2.10 (m, 2 H, SH-CH$_2$-CH_2-CH$_3$), 1.78~1.98 (m, 136 H, -CH-CH_2 in NIPAAm), 1.73 (s, 3 H, SH-CH$_2$-CH$_2$-CH_3), 1.47 (m, 32 H, cyclohexyl-*H*), 1.21~1.38 (m, 108 H, *H*- in t-butyl), 1.06~1.15 (m, 456 H, CH_3-CH-CH_3 in ^{i}PrO- and NIPAAm). GPC (THF): *Mn* = 10953, *Mw* = 11830, PDI = 1.08. α_{25}^D = -14.2 (C = 0.005 g/mL, CH_2Cl_2), titanium content: 0.508 mmol·g^{-1}.

PN$_{66}$(IS)$_6$: FT-IR (KBr): γ_{max}/cm^{-1} 3441, 3309, 3061, 2974, 2927, 2864, 1651, 1530, 1453, 1382, 1363, 1266, 1176, 1123, 1051, 920, 883, 836, 805, 708, 625, 504 cm^{-1}. ^{1}H NMR (500 MHz, CD_3Cl_3): δ 8.13~7.72(m, 12 H, C*H*=N), 7.18~7.69 (m, 24 H, Ar*H*), 6.21~6.92 (m, 66 H, HC-N*H*-C=O), 6.16 (m, 6 H, N-C*H*-CH$_2$- of N-vinyl), 4.04 (m, 6 H, C=NC*H*), 3.97 (m, 66 H, -C*H*-CH$_2$- in NIPAAm), 3.81(m, 6 H, C=NC*H*), 3.56 (m, 24 H, -CH-CH_2- of N-vinyl in IL and -N-CH_2-N-),3.23 (m, 66 H, CH$_3$-C*H*-CH$_3$ in NIPAAm), 3.09 (m, 36 H, -N-CH_2-CH_2-N- and -N-CH_2-Ph-), 2.75(m, 2 H, SH-CH_2-CH$_2$-CH$_3$), 2.41~2.61 (m, 12 H, CH$_3$-C*H*-CH$_3$ of ^{i}PrO- in Ti(salen)), 2.23 (m, 2 H, SH-CH$_2$-CH_2-CH$_3$), 1.76~1.82 (m, 132 H, -CH-CH_2 in NIPAAm), 1.75 (s, 3 H, SH-CH$_2$-CH$_2$-CH_3), 1.41(m, 48 H, cyclohexyl-*H*), 1.22~1.31(m, 162 H, *H*- in t-butyl), 1.01~1.12 (m, 469 H, CH_3-CH-CH_3 in ^{i}PrO- and NIPAAm). GPC (THF): *Mn* = 12160, *Mw* = 13620, PDI = 1.12. α_{25}^D = -16.8 (C = 0.005 g/mL, CH_2Cl_2), titanium content: 0.525 mmol. g^{-1}.

PN$_{64}$(IS)$_8$: FT-IR (KBr): γ_{max}/cm^{-1} 3435, 3302, 3066, 2974, 2924, 2860, 1655, 1535, 1455, 1380, 1365, 1264, 1174, 1125, 1054, 924, 882, 839, 806, 709, 634, 625, 507 cm^{-1}. ^{1}H NMR (500 MHz, CD_3Cl_3): δ 8.11~7.62 (m, 16 H, C*H*=N), 7.13~7.67 (m, 32 H, Ar*H*), 6.24~6.87 (m, 64 H, HC-N*H*-C=O), 6.22 (m, 8 H, N-C*H*-CH$_2$- of N-vinyl), 4.46 (m, 8 H, C=NC*H*), 4.05 (m, 64 H, -C*H*-CH$_2$- in NIPAAm), 3.78 (m, 8 H, C=NC*H*), 3.58 (m, 32 H, -CH-CH_2- of N-vinyl in IL and -N-CH_2-N-), 3.18 (m, 64 H, CH$_3$-C*H*-CH$_3$ in NIPAAm), 2.86 (m, 48 H, -N-CH_2-CH_2-N- and -N-CH_2-Ph-), 2.75(m, 2 H, SH-CH_2-CH$_2$-CH$_3$), 2.45~2.63 (m, 16 H, CH$_3$-C*H*-CH$_3$ of ^{i}PrO- in Ti(salen)), 2.12 (m, 2 H, SH-CH$_2$-CH_2-CH$_3$), 1.75~1.87 (m, 128 H, -CH-CH_2- in NIPAAm), 1.73(s, 3 H, SH-CH$_2$-CH$_2$-CH_3), 1.41 (m, 64 H, cyclohexyl-*H*), 1.22~1.31 (m, 216 H, *H*- in t-butyl), 1.01~1.12 (m, 480 H, CH_3-CH-CH_3 in ^{i}PrO- and NIPAAm). GPC (THF): *Mn* = 13504, *Mw* = 14970, PDI = 1.11. α_{25}^D = -18.0 (C=0.005 g/mL, CH_2Cl_2), titanium content: 0.568 mmol.g^{-1}

Preparation of PN$_{68}$S$_4$: The *IL*-free counterpart of **PN$_{68}$S$_4$**, in which multiple chiral salen Ti^{IV} complexes were directly appended on linear polymer backbone, was also prepared according to a similar procedure to that of **PN$_x$(IS)$_y$**. The chiral salen ligand of (*R,R*)-N-(3,5-di-tert-butylsalicylidene)-N'-[3-tert-butyl-5-vinyl]-1,2-cyclohexanediamine (CL2) treated with Ti(O^{i}Pr)$_4$ was used as the hydrophobic monomer to copolymerize with NIPAAm in the presence of AIBN and *n*-propanethiol, giving the amphiphilic **PN$_{68}$S$_4$** (where the repeated number of NIPAAm units is 64, and the repeated number of Ti(salen) units is 8, as determined by ^{1}H NMR spectrum of the copolymer, see Section S1 in ESI). FT-IR (KBr): γ_{max}/cm^{-1} 3435, 3304, 3077, 2965, 2924, 2868, 1664, 1539, 1457, 1380, 1369, 1268, 1174, 1125, 1050, 967, 926, 880, 835, 806, 708, 679, 507 cm^{-1}. ^{1}H NMR (500 MHz, $CDCl_3$): δ 8.31~7.78 (m, 8 H, C*H*=N), 7.11~7.72 (m, 16 H, Ar*H*), 6.06~6.78 (s, 68 H, HC-N*H*-C=O), 4.76 (s, 4 H, C=NC*H*), 4.09 (s, 68 H, -C*H*-CH$_2$- in NIPAAm), 3.48 (s, 4 H, C=NC*H*), 3.41 (m, 8 H, -CH-CH_2-Ph- in Ti(salen)), 3.19 (m, 68 H, CH$_3$-C*H*-CH$_3$ in NIPAAm), 2.91 (s, 2 H, SH-CH$_2$-CH_2-CH$_3$), 2.72~2.84 (s, 8 H, CH$_3$-C*H*-CH$_3$ of ^{i}PrO- in Ti(salen)), 2.63 (m, 2 H, SH-CH$_2$-CH_2-CH$_3$), 1.73~2.11 (s, 136 H,-CH-CH_2- in NIPAAm), 1.72 (s, 3 H, SH-CH$_2$-CH$_2$-CH_3), 1.59~1.67 (s, 32 H, cyclohexyl-*H*), 1.37~1.51 (108 H, *H*- in t-butyl), 1.07~1.32 (456 H, CH_3-CH-CH_3 in ^{i}PrO- and NIPAAm). GPC (THF): *Mn* = 10830, *Mw* = 13270, PDI = 1.50. α_{25}^D = -12.6 (C=0.005 g/mL, CH_2Cl_2), titanium content: 0.586 mmol.g^{-1}.

General procedure for asymmetric oxidation of sulfides to sulfoxides

Catalytic copolymer (0.5 mol% substrate, based on the titanium content in catalyst) and sulfides (1.0 mmol) were added to H_2O (1 mL) under stirring at 25 °C. H_2O_2 (30 wt%, 1.2 mmol) was then dropwise added within 15 min. The resulting mixture was stirred at room temperature until the reaction was judged to be complete based on GC analysis. Then, the reaction mixture was heated to 80 °C. Catalyst was precipitated out from the reaction system, washed with *n*-hexane (3×5 mL), dried in a vacuum. The supernatants separated from reaction system were extracted with dichloromethane thrice. Combined organic phase was concentrated in vacuum. Further purification of the residue by chromatography on silica gel (petroleum ether/ethyl acetate, 1.5/1) afforded pure sulfoxides. The pure sulfoxides have been identified by ^{1}H and ^{13}C NMR spectra. The conversion and chemoselectivity of chiral sulfoxide were measured by a 6890N gas chromatograph (Agilent Co.) equipped with a capillary column (HP19091G-B213, 30 m × 0.32 mm × 0.25 μm) and a FID detector. Ee values of corresponding chiral sulfoxides were determined by HPLC analysis using the Daicel chiralpak AD columns. Detailed NMR and HPLC analysis for produced sulfoxides were available in Section S2 of ESI.

Methyl phenyl sulfoxide: Chemoselectivity: 95% determined by GC, nitrogen was used as the carrier gas with a flow of 30 mL.min^{-1}, injector temperature and detector temperature were 250 °C, the column temperature was programmed from 80 to 180 °C with 6 °C·min^{-1}, $t_{methyl\ phenyl\ sulfoxide}$ = 6.9 min; ee value: 98% determined by HPLC (*i*-PrOH/*n*-hexane = 1: 9 (v/v)); flow rate = 1.0 mL.min^{-1}; 25 °C; λ = 254 nm; major enantiomer t_R = 18.7 min, minor enantiomer t_S = 21.2 min; ^{1}H NMR ($CDCl_3$, 500 MHz): δ (ppm): 2.55-2.57 (s, 3 H, Me), 7.27-7.38 (m, 3 H, Ar*H*), 7.39-7.51 (m, 2 H, Ar*H*).^{13}C NMR ($CDCl_3$, 125 MHz): δ (ppm): 43.9 (S*C*H$_3$), 123.5, 129.3, 130.9, 145.6(Ar*C*).

Methyl p-bromophenyl sulfoxide: Chemoselectivity: 92% determined by GC, nitrogen was used as the carrier gas with a flow of 30 mL.min^{-1}, injector temperature and detector temperature were 250 °C, the column temperature was 180 °C, $t_{methyl\ p\text{-}bromophenyl\ sulfoxide}$ = 11.2 min; ee value: >99% was determined by HPLC (*i*-PrOH/*n*-hexane = 5:5 (v/v)); flow rate = 1.0 mL min^{-1}; 25 °C; λ = 254 nm; major enantiomer t_R = 8.2 min and minor enantiomer t_S =10.0 min; ^{1}H NMR ($CDCl_3$, 500 MHz): δ (ppm): 3.15 (s, 3 H, SCH_3), 7.74-7.76 (d, 2 H, Ar*H*), 7.83-7.84 (d, 2 H, Ar*H*).^{13}C NMR ($CDCl_3$, 125 MHz): δ (ppm): 44.5 (S*C*H$_3$), 125.3, 129.1, 132.8, 139.6(Ar*C*).

View Article Online
DOI: 10.1039/C6GC02743A

Methyl p-methoxyphenyl sulfoxide: Chemoselectivity: 94% determined by GC, nitrogen was used as the carrier gas with a flow of 30 mL.min^{-1}, injector temperature and detector temperature were 250 °C, the column temperature was programmed from 80 to 180 °C with 6 °C·min^{-1}, $t_{methyl\ p\text{-}methoxyphenyl\ sulfoxide}$ = 11.7 min; ee value: 95% determined by HPLC (*i*-PrOH/*n*-hexane = 2:8 (v/v)); flow rate = 1.0 mL.min^{-1}; 25 °C; λ = 254 nm; major enantiomer t_R = 8.9 min and minor enantiomer t_S = 10.2 min; ^{1}H NMR ($CDCl_3$, 500 MHz): δ (ppm): 3.07 (s, 3 H, SC*H*$_3$), 3.95 (s, 3 H, OC*H*$_3$), 7.06-7.10 (d, 2 H, Ar*H*), 7.84-7.91 (d, 2 H, Ar*H*). ^{13}C NMR ($CDCl_3$, 125 MHz): δ (ppm): 44.8 (S*C*H$_3$), 55.8 (O*C*H$_3$), 114.6, 129.6, 132.3, 163.7 (Ar*C*).

Methyl p-nitrophenyl sulfoxide: Chemoselectivity: 98% determined by GC, nitrogen was used as the carrier gas with a flow of 30 mL.min^{-1}, injector temperature and detector temperature were 250 °C, the column temperature was 180 °C, $t_{methyl\ p\text{-}nitrophenyl\ sulfoxide}$ = 8.6 min; ee value: 88% determined by HPLC (*i*-PrOH/*n*-hexane = 3:7 (v/v)); flow rate = 1.0 mL.min^{-1}; 25 °C; λ = 254 nm; major enantiomer t_R = 11.5 min and minor enantiomer t_S =21.5 min; ^{1}H NMR ($CDCl_3$, 500 MHz): δ (ppm): 2.59 (s, 3H, SC*H*$_3$), 7.27-7.42 (d, 2H, Ar*H*), 8.09-8.20 (d, 2H, Ar*H*).^{13}C NMR ($CDCl_3$, 125 MHz): δ (ppm): 43.8 (S*C*H$_3$), 123.9, 124.9, 144.7, 148.8 (Ar*C*).

Methyl o-methoxyphenyl sulfoxide: Chemoselectivity: 90% determined by GC, nitrogen was used as the carrier gas with a flow of 30 mL.min^{-1}, injector temperature and detector temperature were 250 °C, the column temperature was 180 °C, $t_{methyl\ o\text{-}methoxyphenyl\ sulfoxide}$ = 9.8 min; ee value: >99% determined by HPLC (*i*-PrOH/*n*-hexane = 2:8 (v/v)); flow rate = 1.0 mL.min^{-1}; 25 °C; λ = 254 nm; major enantiomer t_R = 9.0 min and minor enantiomer t_S =10.3 min; ^{1}H NMR ($CDCl_3$, 500 MHz): δ (ppm): 2.68 (s, 3 H, SC*H*$_3$), 3.78 (s, 3 H, OC*H*$_3$), 6.79-7.90 (m, 4 H, Ar*H*).^{13}C NMR ($CDCl_3$, 125 MHz): δ (ppm): ^{13}C NMR ($CDCl_3$, 125 MHz): δ (ppm): 41.1 (S*C*H$_3$), 55.7 (O*C*H$_3$), 110.5, 121.5, 124.4, 132.0, 132.8, 154.7 (Ar*C*).

Ethyl phenyl sulfoxide: Chemoselectivity: 97% determined by GC, nitrogen was used as the carrier gas with a flow of 30 mL. min^{-1}, injector temperature and the detector temperature were 250 °C, the column temperature was 180 °C, $t_{ethyl\ phenyl\ sulfoxide}$ = 2.5 min; ee value: >99% determined by HPLC (*i*-PrOH/ *n*-hexane = 1: 9 (v/ v)); flow rate = 1.0 mL. min^{-1}; 25 °C; λ = 254 nm; major enantiomer t_R = 8.2 min. ^{1}H NMR ($CDCl_3$, 500 MHz): δ (ppm): 1.18 (m, 3 H, Me), 2.90-2.98 (m, 2 H, -C*H*$_2$-), 7.28-7.29 (m, 1 H, Ar*H*), 7.33-7.49 (m, 2 H, Ar*H*), 7.50-7.62 (m, 2 H, Ar*H*). ^{13}C NMR ($CDCl_3$, 125 MHz): δ (ppm): 5.90 (*C*H$_3$), 50.23 (S*C*H$_2$), 124.12, 128.76, 129.08, 145.87 (Ar*C*).

n-Butyl phenyl sulfoxide: Chemoselectivity: >99% determined by GC, nitrogen was used as the carrier gas with a flow of 30 mL. min^{-1}, injector temperature and the detector temperature were 250 °C, the column temperature was 180 °C, $t_{n\text{-}butyl\ phenyl\ sulfoxide}$ = 2.9 min; ee value: >99% determined by HPLC (i-PrOH/ *n*-hexane = 1: 9 (v/v)); flow rate = 1.0 mL. min^{-1}; 25 °C; λ = 254 nm; major enantiomer t_R = 9.2 min. ^{1}H NMR ($CDCl_3$, 500 MHz): δ (ppm): 0.90-0.93 (m, 3 H, Me), 1.41-1.48 (m, 2 H,-C*H*$_2$-), 1.60-1.67 (m, 2 H,-C*H*$_2$-), 2.90-2.93 (m, 2 H,-C*H*$_2$-), 7.15-7.16 (m, 1 H, Ar*H*), 7.24-7.26 (m, 2 H, Ar*H*), 7.28-7.31 (m, 2 H, Ar*H*). ^{13}C NMR ($CDCl_3$, 125 MHz): δ (ppm): 13.52 (*C*H$_3$), 21.86 (*C*H$_2$), 31.13 (*C*H$_2$), 58.12 (*C*H$_2$), 125.56, 128.72, 128.77, 136.91 (Ar*C*).

n-Hexyl phenyl sulfide: Chemoselectivity: >99% determined by GC, nitrogen was used as the carrier gas with a flow of 30 mL.min^{-1}, injector temperature and the detector temperature were 250 °C, the column temperature was 180 °C, $t_{n\text{-}hexyl\ phenyl\ sulfoxide}$ = 4.3 min; ee value: >99% determined by HPLC (i-PrOH/ *n*-hexane = 1: 9 (v/v)); flow rate = 1.0 mL. min^{-1}; 25 °C; λ = 254 nm; major enantiomer t_R = 17.5 min. ^{1}H NMR ($CDCl_3$, 500 MHz): δ (ppm): 0.87-0.90 (s, 3 H, Me), 1.26-1.68 (m, 4 H,-C*H*$_2$- C*H*$_2$-), 1.66-1.69 (m, 2 H, -C*H*$_2$-), 2.89-2.93 (m, 2 H, -C*H*$_2$-), 7.15-7.16 (m, 1 H, Ar*H*), 7.25-7.28 (m, 2 H, Ar*H*), 7.31-7.32 (m, 2 H, Ar*H*). ^{13}C NMR ($CDCl_3$, 125 MHz): δ (ppm): 14.04 (*C*H$_3$), 22.55 (*C*H$_2$), 28.54 (*C*H$_2$), 31.38 (*C*H$_2$), 33.60 (*C*H$_2$), 58.21 (*C*H$_2$), 125.62, 128.80, 128.85, 137.08 (Ar*C*).

Sulfoxidation reaction for kinetic measurement

Catalyst (0.5 mol% of substrate, based on titanium ion content in copolymer) was stirred with methyl phenyl sulfide (1.0 mmol) in deionized water (1 mL) at 25 °C. H_2O_2 (30 wt%, 1.2 mmol) was then added into the mixture in one portion. To determine the rate of sulfoxidation, aliquots at an interval of 5 min were drawn from the reaction mixture, filtrated through silica gel with ethyl acetate as an eluent and analyzed by GC.

Acknowledgements

The work was supported by the National Natural Science Foundation of China (21476069, 21676078), the Natural Science Foundation of Hunan Province for Distinguished Young Scholar (2016JJ1013), the Scientific Research Fund of Hunan Provincial Education Department (13B072), and the Program for Excellent Talents in Hunan Normal University (ET14103). The authors are grateful to Prof. Linpeng Cheng and Bin Xu (Tsinghua University) for their help with the characterization using Cryo-TEM at Tsinghua University Branch of the National Center for Protein Sciences (Beijing).

Notes and references

[1] a) T. Tanaka, B. Saito and T. Katsuki, *Tetrahedron Lett.,* 2002, **43**, 3259; b) B. Ferber and H. B. Kagan, *Adv. Synth. Catal.,* 2007, **349**, 493; c) M. A. Fascione, S. J. Adshead, P. K. Mandal, C. A. Kilner, A. G. Leach and W. B. Turnbull, *Chem. Eur. J.,* 2012, **18**, 2987; d) H. Srour, P. L. Maux, S. Chevance and G. Simonneaux, *Coord. Chem. Rev.,* 2013, **257**, 3030; e) W. Xuan, C. Ye, M. Zhang, Z. Chen and Y. Cui, *Chem. Sci.,* 2013, **4**, 3154.

[2] a) M. Garcia-Viloca, J. Gao, M. Karplus and D. G. Truhlar, *Science,* 2004, **303**, 186; b) A. Warshel, *Angew. Chem. Int. Ed.,* 2014, **53**, 10020.

[3] a) M. Ouchi, N. Badi, J. F. Lutz and M. Sawamoto, *Nat. Chem.,* 2011, **3**, 917; b) T. Terashima, T. Mes, T. F. A. De Greef, M. A. J. Gillissen, P. Besenius, A. R. A. Palmans and E. W. Meijer, *J. Am. Chem. Soc.,* 2011, **133**, 4742; c) N. Hosono, M. A. J. Gillissen, Y. Li, S. S. Sheiko, A. R. A. Palmans and E. W. Meijer, *J. Am. Chem. Soc.,* 2013, **135**, 501; d) Y. Liu, T. Pauloehrl, S. I. Presolski, L. Albertazzi, A. R. A. Palmans and E. W. Meijer, *J. Am. Chem. Soc.,* 2015, **137**, 13096; e) M. Gonzalez-Burgos, A. Latorre-Sanchez and J. A. Pomposo, *Chem. Soc. Rev.,* 2015, **44**, 6122.

[4] a) N. Giuseppone and J. F. Lutz, *Nature,* 2011, **473**, 40; b) M. A. J. Gillissen, T. Terashima, E. W. Meijer, A. R. A. Palmans and I. K. Voets, *Macromolecules,* 2013, **46**, 4120; c) P. J. M. Stals, C. Cheng, L. van Beek, A. C. Wauters, A. R. A. Palmans, S. Han and E. W. Meijer, *Chem. Sci.,* 2016, **7**, 2011.

[5] a) M. A. Gauthier, M. I. Gibson and H.-A. Klok, *Angew. Chem. Int. Ed*., 2009, **48**, 48; b) D. M. Stevens, S. Tempelaar, A. P. Dove and E. Harth, *ACS Macro. Lett.,* 2012, **1**, 915; c) A. Sanchez-Sanchez, D. A. Fulton and J. A. Pomposo, *Chem. Commun.,* 2014, **50**, 1871; d) G. M. ter Huurne, M. A. J. Gillissen, A. R. A. Palmans, I. K. Voets and E.W. Meijer, *Macromolecules,* 2015, **48**, 3949.

[6] a) Y. N. Belokon, M. North, V. I. Maleev, N. V. Voskoboev, M. A. Moskalenko, A. S. Peregudov, A. V. Dmitriev, N. S. Ikonnikov and H. B. Kagan, *Angew. Chem. Int. Ed.,* 2004, **43**, 4085; b) R. M. Haak, S. J. Wezenberg and A. W. Kleij, *Chem. Commun.,* 2010, **46**, 2713; c) Y.

View Article Online
DOI: 10.1039/C6GC02743A

Zhang, R. Tan, G. Zhao, X. Luo, C. Xing and D. Yin, *J. Catal.,* 2016, **335**, 62.
[7] a) C. E. Song and E. J. Roh, *Chem. Commun.,* 2000, **10**, 837; b) R. Tan, D. Yin, N. Yu, H. Zhao and D. Yin, *J. Catal.,* 2009, **263**, 284; c) R. Luo, R. Tan, Z. Peng, W. Zheng, Y. Kong and D. Yin, *J. Catal.,* 2012, **287**, 170; d) G. Zhao, R. Tan, Y. Zhang, X. Luo, C. Xing and D. Yin, *RSC Adv.,* 2016, **6**, 24704.
[8] A. A. Gridnev, C*hem. Rev.,* 2001, **101**, 3611.
[9] A. Lu and R. K. O'Reilly, *Curr. Opin. Biotechnol*., 2013, **24**, 639.
[10] T. Terashima, T. Sugita, K. Fukae and M. Sawamoto, *Macromolecules*, 2014, **47**, 589.
[11] M. Holbach, X. Zheng, C. Burd, C. W. Jones and M. Weck, *J. Org. Chem.,* 2006, **71**, 2903.
[12] K. Yu, Z. Gu, R. Ji, L. Lou and S. Liu, *Tetrahedron,* 2009, **65**, 305.
[13] J. Kim and K. Geon-Joong, *Catal. Lett*., 2004, **92**, 123.
[14] C. Lv, D. Xu, S. Wang, C. Miao, C. Xia and W. Sun, *Catal. Commun.,* 2011, **12**, 1242.
[15] F. Song, C. Wang, J. M. Falkowski, L. Ma and W. Lin, *J. Am. Chem. Soc.,* 2010, **132**, 15390.
[16] Y. Liu, T. Pauloehrl, S. I. Presolski, L. Albertazzi, A. R. A. Palmans and E. W. Meijer, *J. Am. Chem. Soc.,* 2015, **137**, 13096.
[17] T. Sun and G. Qing, *Adv. Mater*., 2011, **23**, 57.
[18] a) M. Li, S. Qi, Y. Jin, W. Yao, S. Zhang and J. Zhao, *Colloids Surf. B,* 2014, **123**, 852; b) Y. Zhang, R. Tan, G. Zhao, X. Luo and D. Yin, *Catal. Sci. Technol.,* 2016, **6**, 488.
[19] X. Huang, Y. Xiao and M. Lang, *J. Colloid Interface Sci.,* 2011, **364**, 92.
[20] L. Schoonen and J. C. M. van Hest, *Adv. Mater*., 2016, **28**, 1109.
[21] a) Q. Fan, Y. Li and A. S. C. Chan, *Chem. Rev.,* 2002, **102**, 3385; b) B. Helms and J. M. J. Frichet, *Adv. Synth. Catal.,* 2006, **348**, 1125.
[22] a) Y. Gu and G. Li, *Adv. Synth. Catal.,* 2009, **351**, 817; b) J. Long, W. Lou, L. Wang, B. Yin and X. Li, *Chem. Eng. Sci.,* 2015, **122**, 24.
[23] J. Lu, L. Liang and M. Weck, *J. Mol. Catal. A: Chem.,* 2016, **417**, 122.
[24] S. colonna, R. fornasier. *Synthesis*, 1975, **8**, 531.
[25] T. Dwars, E. Paetzold and G. Oehme, *Angew. Chem. Int. Ed*., 2005, **44**, 7174.
[26] K. Renggli, P. Baumann, K. Langowska, O. Onaca, N. Bruns, W. Meier, *Adv. Funct. Mater*., 2011, **21**, 1241.
[27] C. Baleizaõ and H. Garcia, *Chem. Rev*., 2006, **106**, 3987.

View Article Online
DOI: 10.1039/C6GC02743A

Graphical Abstract

Bio-inspired single-chain polymeric nanoparticles containing chiral salen Ti^{IV} complex for highly enantioselective sulfoxidation in water

Yaoyao Zhang, Rong Tan,* Mengqiao Gao, Pengbo Hao and Donghong Yin

Key Laboratory of Chemical Biology and Traditional Chinese Medicine Research (Ministry of Education); National & Local Joint Engineering Laboratory for New Petro-chemical Materials and Fine Utilization of Resources, Hunan Normal University, Changsha 410081 (P. R. China)

Bio-inspired SCPNs containing chiral salen Ti^{IV} complex in *IL*-mediated hydrophobic cavity exhibited enzyme-mimetic activity and selectivity in aqueous enantioselective sulfoxidation.

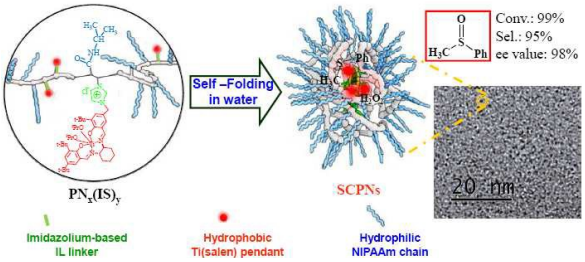

* Corresponding authors. Fax: +86-731-8872531. Tel: +86-731-8872576

E-mail: yiyangtanrong@126.com